Proceedings of the 26th Annual International Conference of the IEEE EMBS
San Francisco, CA, USA • September 1-5, 2004

Analyses of Rotational Singularities in Ferret Visual Cortex

Vidyasagar Vasamsetty[1], David M.Coppola[2], Charles J.Robinson[3, 5], Kerrie Tainter[4], Ben Choi[1]
[1]Dept of Computer Science, Louisiana Tech Univ.; [2]Dept of Biology, Centenary College; [3]Cntr for Biomedical Engineering & Rehab Science, Louisiana Tech Univ.; [4]Biomedical Research Institute, Shreveport, LA; [5]Shreveport VA Medical Center

Abstract— **Activity maps of spatial orientation, obtained by intrinsic optical imaging of the mammalian visual cortex, show the formation of pinwheel-like structures that rotate either clockwise or counterclockwise around zero dimensional points called singularities. Any research that is oriented towards exploring the formation and physiological role of these singularities during an experiment requires an automated tool that can rapidly identify the location of these singularities. In this work we have developed such a tool that looks for the existence of singularities for a certain radius at every pixel location in the angle map. Using data from eleven ferrets, the number of singularities identified was a function of the search radius (0.03325, 0.04665, 0.05985, 0.07315, 0.08645, 0.09975, 0.11305, and 0.12635 mm) and level of image smoothing used. For a given smoothing value, the number of singularities decreased with increasing radius. But the rate of decrease was greater with less smoothing. The more the original image was smoothed, the fewer singularities were identified at a given radius. The trade off between search radius and image smoothing can be partially attributed to spatial sampling resolution.**

Keywords—**Singularity, pinwheel center, orientation preference, visual cortex neurophysiology, image processing**

I. Introduction

Many neurons in mammalian primary visual cortex respond selectively to a particular orientation of visual stimulus. The orientation preference is constant for perpendicular penetrations of microelectrodes and can be characterized by a continuous rotation for lateral penetrations of microelectrodes [1, 2]. Based on these observations Huble and Wiesel proposed a columnar organization for the cortex, with each column exhibiting a particular preferential orientation. Prior to their findings, research exploring the functional brain architecture using microelectrodes was focused on single neurons or at most two or three neurons at a time. Intrinsic and Extrinsic optical imaging techniques are a promising method for monitoring neuronal populations' response properties with high spatial and temporal resolution.

Activity maps obtained by *in vivo* Intrinsic Optical Imaging of the mammalian cortex responding to visual stimulus, a moving bar grating of 0°, 45°, 90° and 135° orientation, revealed the formation of 'iso-orientation domains:' neighboring groups of cells with similar orientation preference [4, 5]. Different domains often rotate around particular points called 'orientation centers' [4] either in clockwise or counterclockwise directions.

These optical activity maps can be converted to vectors [6, 7], and vectorially summed pixel-by-pixel maps give a resultant vector, in which the orientation center become the point where the direction of field vector is not defined. Such points are referred to as singularities in the direction fields and are of two types: clockwise or counterclockwise. When traversed thru an imaginary circle assumed around a singularity in a counterclockwise direction, the vector directions each point along the circle also rotate. They rotate once positively in the case of clockwise singularity and negatively in the case of counterclockwise singularity for each complete traversal of the circle. The singularities are represented by +1 and -1 if they cover a full range of angles from 0° to 360°; or +1/2 and -1/2 if they cover half range i.e. from 0° to 180° [8, 9]. If the resultant vector angles are then color-coded, the angle of best response yields a pinwheel-like structure around the orientation center. The Existence of all four (or eight) orientations each appearing only once around the center, is a property of these pinwheels.

The role of the orientation center or singularity in the processing of visual information has been of long standing debate. Any research exploring the orientation centers requires the use of both the optical imaging techniques and microelectrode recording techniques [10]. Activity maps *vector summed and the resultant vector angles color-coded) reveal the pinwheel centers. One can then test for the physiological aspects of the orientation centers by penetrating a microelectrode at the cortical locations corresponding to the pinwheel centers in the color-coded orientation preference maps. A tool which automates the detection the singularity locations aids significantly in the process. We have developed such a tool in MATLAB using the inbuilt features of the Image Processing Tool Box. The algorithm is described in detail in the methods section. The ferret cortex optical imaging data was obtained from Coppola and White [11, 12] and used with their permission. The effect of different levels of smoothing of the raw data on counts of clockwise and counterclockwise singularities was studied.

II. Methodology

Coppola et al [10], obtained data from eleven ferrets by optical recording of intrinsic signals [6, 7] using standard procedures [3]. Ferrets were given the visual stimulus of four bar gratings oriented at 0°, 45°, 90° and 135° with respect to horizontal. Two sets of orthogonal gratings were presented randomly. One set consisted of the orthogonal pair 0°/90° or 45°/135° and the other set consisted of the orthogonal pair 90°/0° or 135°/45°. The images acquired during the presentation of one grating were summed and then subtracted from the summed images acquired during the presentation of orthogonal grating to create differential maps of orientation preferences (i.e. difference images) for each set of trials. Thus two difference images, which measured

655 X 480 pixels at a scale of 75 pixels per millimeter, were generated from each stimulus pair, making a total of four difference images (i.e., 0°-90°, 45°-135°, 90°-0°, and 135°-45°) per experiment. The remainder of this paper deals with a novel method to analyze the data.

Analytical Treatment

Let DI_{OR}^{0-90}, DI_{OR}^{45-135}, DI_{OR}^{90-0}, and DI_{OR}^{135-45} be the difference images (of size $m \times n$) mentioned above, where OR signifies orientation. These matrices are subjected to a four-step analysis. Steps 2 and 3 are described elsewhere [14, 15].

Step 1. Smoothing and Filtering

The raw spatial images are Gaussian low pass filtered in the frequency domain. Using the following equation:

$$H(u,v) = \exp(-D^2(u,v)/2\sigma^2). \quad (1)$$

Where D (u, v) is the distance from the origin of the Fourier transform and σ is a variable parameter that determines the amount of 2-dimensional smoothing applied.

Step 2. Compute maps

For the ***vector sum*** map, let D_{OR}^{0-90}, D_{OR}^{45-135}, D_{OR}^{90-0} and D_{OR}^{135-45} be the Gaussian smoothed raw data. The difference images are converted to vectors with the angles multiplied by two.

$$D_{OR}^{0-90}(\vec{r}) = D_{OR}^{0-90}\left[\cos(2\times 0°) + i\cdot\sin(2\times 0°)\right] \quad (2)$$

$$D_{OR}^{45-135}(\vec{r}) = D_{OR}^{45-135}\left[\cos(2\times 45°) + i\cdot\sin(2\times 45°)\right] \quad (3)$$

$$D_{OR}^{90-0}(\vec{r}) = D_{OR}^{90-0}\left[\cos(2\times 90°) + i\cdot\sin(2\times 90°)\right] \quad (4)$$

$$D_{OR}^{135-45}(\vec{r}) = D_{OR}^{135-45}\left[\cos(2\times 135°) + i\cdot\sin(2\times 135°)\right]$$

Computing the vector sum of (2), (3), (4), and (5) gives

$$O(\vec{r}) = D_{OR}^{0-90}(\vec{r}) + D_{OR}^{45-135}(\vec{r}) + D_{OR}^{90-0}(\vec{r}) + D_{OR}^{135-45}(\vec{r}). \quad (6)$$

Using polar coordinates equation (6) can be represented as

$$O(\vec{r}) = q(\vec{r})\exp(i\theta). \quad (7)$$

where $\theta = 2\phi(\vec{r})$, (8)

$\phi(\vec{r})$ is the *preferred orientation* and $q(\vec{r})$ is the *orientation tuning strength* of the resultant vector field magnitude.

The '*Angle Map*' [14] AM is given by

$$AM = \begin{cases} \theta & if \quad \theta \geq 0 \\ 360 + \theta & if \quad \theta < 0 \end{cases} \quad (9)$$

The '***Condition Map***' CM [14] is given by

$$CM = floor\left(\frac{AM \times (255/360)}{64}\right) \quad (10)$$

CM is scaled to generate the values 0, 1, 2, and 3 indicating orientation preferences for 0°, 45°, 90°, and 135° respectively.

The ***'Polar Map'*** [15] PM, which considers the preferred orientation and magnitude together, is given by

$$PM = \frac{CM \times 256 + q(\vec{r})}{4} \quad (11)$$

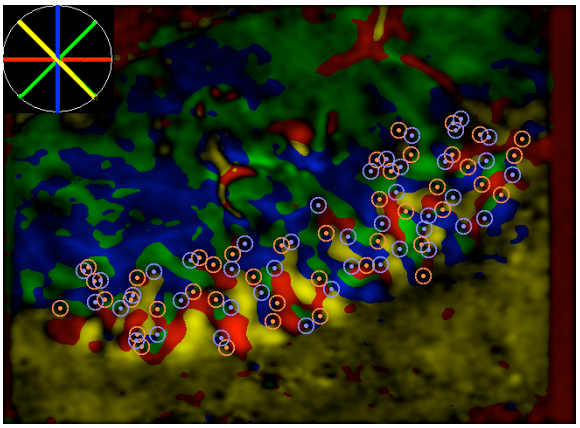

Fig. 1. Polar map of animal F97 with smoothing σ = 28 and radius = 4.5 pixels. False color is used to indicate cardinal and oblique stimulus directions. Singularities are noted by dots surrounded by circles of 9.5 pixel radius (orange for CW; purple for CCW).

Step 3. Find the possible candidates for singularities

This paper now expands the analysis beyond steps 1 and 2. Since θ ranges from 0° to 360°, the singularities in the resultant vector field are represented by either +1, if it is clockwise singularity, or -1, if it is a counterclockwise singularity. The position of the possible candidates for singularities can be determined by computing the sum of all the orientation differences at a certain radius *r=2.5* pixels in clockwise direction around ever pixel in the angle map [13]. If the sum is +360 the pixel is marked as a possible candidate for clockwise singularity. If the sum is -360 the pixel is marked as a possible candidate for counterclockwise singularity. The radius was fixed at 2.5, which is the lowest resolution possible, thus covering all possible singularities occurring at other radii.

Let NP_r be the set of ordinal "*o*" coordinate points at a radius *r* pixels in clockwise direction, such that:

$$NP_r = \sum_{\theta=0}^{2\pi} \begin{pmatrix} x = r + r\cos\theta \\ y = r + r\sin\theta \end{pmatrix} \quad (12)$$

For each and every pixel *(i, j)* in the angle map, where *i* takes the values from 1 to *m* and *j* takes the values from 1 to *n*, one can compute the sum of orientation differences with radius r = 2.5 pixels.

$$OD(i,j) = \sum_{k=1}^{o} \left(AM_{i,j}(NP_r(k)) \otimes AM_{i,j}(NP_r(k+1)) \right) + AM_{i,j}(NP_r(o)) \otimes AM_{i,j}(NP_r(1))$$

The operation $a \otimes b$ is then defined as follows

$$a \otimes b = \begin{cases} a - b - 360 & if \quad |a-b| > |360 - |a-b|| \\ a - b + 360 & if \quad |a-b| \le |360 - |a-b|| \end{cases} \quad (14)$$

Possible candidates for clockwise singularities are given by

$$CW(i,j) = \begin{cases} 1 & if \quad OD(i,j) = +360 \\ 0 & if \quad OD(i,j) \neq +360 \end{cases} \quad (15)$$

Possible candidates for counterclockwise singularities are given by

$$CCW(i,j) = \begin{cases} 1 & if \quad OD(i,j) = -360 \\ 0 & if \quad OD(i,j) \neq -360 \end{cases} \quad (16)$$

The objects in the binary images *CW* and *CCW* are labeled using the pixel connectivity algorithm and the centroid of each of these objects is calculated.

Step 4. Verify and filter unwanted candidates

Let C_c and AC_c be the set of centroids of the possible candidates for clockwise and counterclockwise singularities obtained with r equal 2.5 pixels. Let n_c and n_{ccw} be the cardinality of C_c and AC_c. In order to determine whether a coordinate in C_c and AC_c, is a true singularity at a certain radius r', the following two conditions must be satisfied.

1. In the angle map the sum of orientation differences around the coordinate points in C_c (or AC_c) should be +360 (or -360).

One must therefore evaluate NP_r at radius $r=r'$ for all (x, y) belonging to C_c,

$$CL = \left\{ (x,y) \text{ if } \sum_{k=1}^{o} \left(AM_{x,y}(NP_r(k)) \otimes AM_{x,y}(NP_r(k+1)) \right) + AM_{x,y}(NP_r(o)) \otimes AM_{x,y}(NP_r(1)) = 360 \right\}$$

for a clockwise singularity

OR

evaluate NP_r at radius $r=r'$ for all (x, y) belonging to AC_c.

$$CCL = \left\{ (x,y) \text{ if } \sum_{k=1}^{o} \left(AM_{x,y}(NP_r(k)) \otimes AM_{x,y}(NP_r(k+1)) \right) + AM_{x,y}(NP_r(o)) \otimes AM_{x,y}(NP_r(1)) = -360 \right\}$$

for a counterclockwise singularity.

2. All four conditions (or angles) should exist at radius r'.

Let Q be the set of all conditions at a radius r' in the condition map, for all (x, y) belonging to *CL (or CCL)*.

$$Q = CM_{x,y}(NP_r(k)) . \quad (19)$$

One must test for the existence of all four values 0, 1, 2, and 3 in Q; i.e. preference for the orientations 0°, 45°, 90° and 135°.

III. Results

Before applying step 3 of the algorithm, a region of interest was selected manually to narrow the search, thus excluding regions, such as map borders, outside the area of interest. The singularities obtained were plotted with in a radius of 9.5 pixels. Fig.1 shows the clockwise and counterclockwise Singularity plots of F97 ferret data for σ = 28 and radius = 4.5 pixels.

To study the effect of smoothing and radius choice on the number of singularities, the algorithm is applied at different smoothing levels (i.e. the σ parameter in Gaussian low pass filter is varied) and radii. Fig 2 shows two extremes: F97 where plot lines are parallel and F82 where slopes converge.

IV. Discussion

From the figures we observe that a large number of singularities are common for all radii. These types of singularities are mostly isotropic in nature; i.e., all four conditions share almost equal area within a particular radius. There are few singularities that show up at one particular radius and not at other radii. This may be because of the anisotropic nature of such singularities. Trade offs exists between smoothing (_ value) of raw data and the spatial resolution (count of singularities) as radius r is increased (i.e., decreasing the spatial sample frequency). Such an observation can be attributed to frequency sampling limitations.

Since singularities can occur at any radius, it can be concluded that there is no fixed radius that will capture all possible singularities. On the one hand, extreme smoothing of the raw data will not reveal all the existing singularities. On the other hand, choosing the largest radius for analysis could possibly obscure potential singularities.

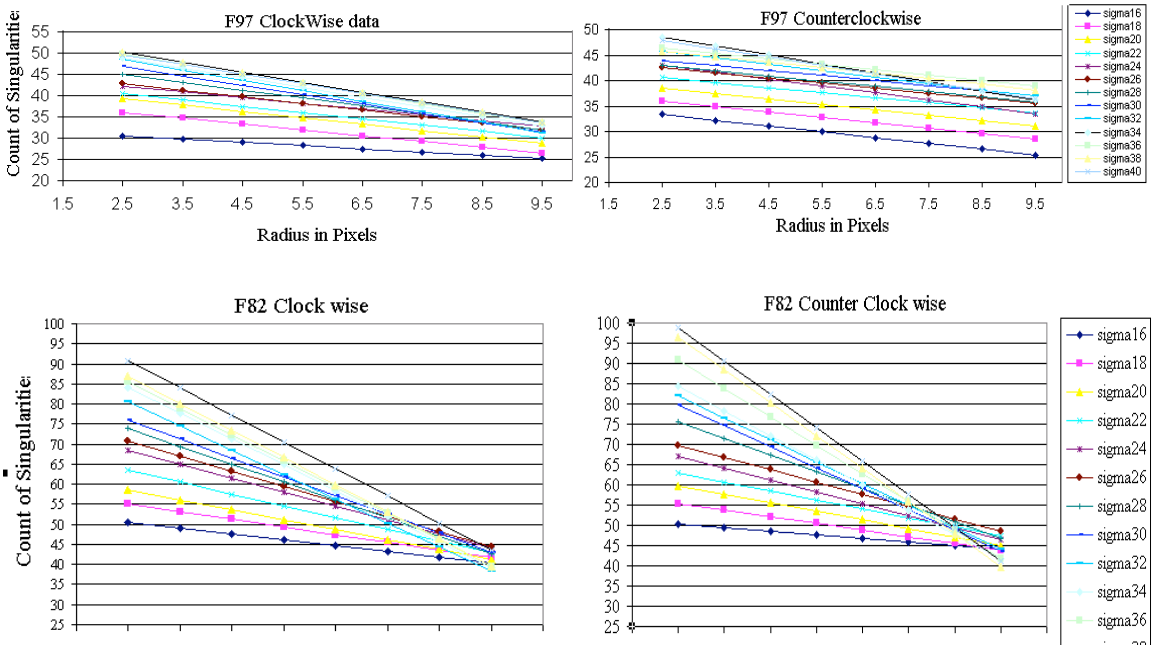

Fig. 2: Plots of # of singularities versus radius r & smoothing σ. The lower the value of σ, the more the amount of smoothing. A larger radius captures a bigger portion of the image in which to look for a singularity.

The results from the two animals plotted at the same scale represent the extremes of the tradeoff between #, r, and σ.

A desirable smoothing level could be experimentally dependent, and best determined before processing the raw data. Orientations change smoothly around the singularity points, but there may be points called fractures around which the orientation preference changes by up to 90° and vortices where orientation preferences rotate through a complete cycle of 180°. These points fall within certain linear zones of the visual cortex. The tool can not distinguish between whether a point is a zero dimensional singularity or a one-dimensional fracture [7].

Techniques have been demonstrated that yield tradeoff between 2-dimensional smoothing of raw image verses the choice of a radius in which to search for singularities.

V. Acknowledgments

The authors thank Leonard E. White for permission to use the ferret visual cortex data.

VI. References

[1] D. H. Hubel, T. N. Wiesel, "Sequence regularity and geometry of orientation columns in the monkey striate cortex," *J Comp Neurol.,* vol. 158, pp.267-293,1974.

[2] D. H. Hubel, T. N. Wiesel, "Uniformity of monkey striate cortex: a parallel relationship between field size, scatter and magnification factor," *J Comp Neurol.,* vol. 158, pp.295-306, 1974.

[3] T. Bonhoeffer and A. Grinvald, "The Methods," in *Brain Mapping*, A. Toga and J. C. Mozziotta, San Diego, CA: Academic Press, 1996, pp.55-97.

[4] T. Bonhoeffer and A. Grinvald, "The layout of iso-orientation domains in area 18 of cat visual cortex: Optical imaging reveals a pinwheel-like organization," *J. Neurosci.,* vol. 13, pp.4157-4180, 1993.

[5] T. Bonhoeffer, and A. Grinvald, "Iso-orientation domains in cat visual cortex are arranged in pinwheel-like patterns," *Nature,* vol. 353, pp.429-431, Oct.1991.

[6] G. G. Blasdel, "Differential imaging of ocular dominance and orientation selectivity in monkey striate cortex," *J Neurosci.,* vol. 12, pp.3115-3138, 1992.

[7] G. G Blasdel, "Orientation Selectivity, preference and continuity in monkey striate cortex," *J Neurosci*., vol. 12, pp3139-3161,1992.

[8] R. Penrose, "The topology of ridge systems," *Ann. Hum Genet*., vol. 42, pp.435-444, 1979.

[9] N. V, Swindale, "Visual cortex: Looking into a klein bottle", *Current Biology*, vol. 6, pp 7:776-779, 1996.

[10] P.E.Maldonado, I. Gödecke, C. M. Gray, T, "Orientation selectivity in pinwheel centers in cat striate cortex", *Science*, vol. 276, pp.1551-1555. June 1997.

[11] David M. Coppola, Leonard E. White, David Fitzpatrick, and Dale Purves., "Unequal representation of cardinal and oblique contours in ferret visual cortex," *Proc. Natl. Acad. Sci.,* USA., vol. 95, pp.2621-2623, Mar 1998.

[12] Leonard E. White, David M. Coppola & David Fitzpatrick., "The contribution of sensory experience to the maturation of orientation selectivity in ferret visual cortex," *Nature*, vol. 411, pp.1049-1052, June 2001.

[13] K. Obermayer, G.G. Blasdel, "Singularities in primate orientation maps," *Neural Computation,* vol. 9, pp.555-575, April 1997.

[14] G. G. Blasdel and G. Salama , " Voltage-sensitive dyes reveal a modular organization in monkey striate cortex", *Nature*, vol. 321, pp.579-589, 1986.

[15] D. Y. Ts'o, R. D. Frostig, E. Lieke, A. Grinvald, "Functional organization of primate visual cortex revealed by high resolution optical imaging," *Science,* vol. 249, pp.417-420, 1990.